2008

Source Mechanisms Of Terrestrial Gamma-ray Flashes

Joseph R. Dwyer

Source mechanisms of terrestrial gamma-ray flashes

J. R. Dwyer[1]

Received 2 August 2007; revised 7 November 2007; accepted 10 January 2008; published 20 May 2008.

[1] The source of terrestrial gamma-ray flashes (TGFs) has remained a mystery since their discovery in 1994. Recent Reuven Ramaty High-Energy Solar Spectroscopic Imager (RHESSI) observations show that these intense bursts of MeV gamma rays likely originate much deeper in the atmosphere than previously inferred from Burst and Transient Source Experiment (BATSE) data, with the source altitude <21 km. Using existing measurements of the intensity and duration of BATSE and RHESSI TGFs, along with limits on the electric field set by the relativistic feedback mechanism involving backward propagating positrons and x-rays, it is found that TGFs cannot be produced by relativistic runaway electron avalanches acting on natural background radiation or extensive cosmic-ray air showers alone, as has been assumed by many previous models. Instead, the energetic seed particle production most likely involves either relativistic feedback or runaway electron production in the strong electric fields associated with lightning leaders or streamers, similar to the energetic radiation observed on the ground from lightning.

Citation: Dwyer, J. R. (2008), Source mechanisms of terrestrial gamma-ray flashes, *J. Geophys. Res.*, *113*, D10103, doi:10.1029/2007JD009248.

1. Introduction

[2] Despite over a decade of research, the sources of terrestrial gamma-ray flashes (TGFs) remain a mystery. Not only are the exact source locations unknown, the basic mechanism for producing the energetic electrons that emit the high-energy photons is still under active debate. When TGFs were first reported using data from the Burst and Transient Source Experiment (BATSE) on NASA's Compton Gamma-Ray Observatory (CGRO) [*Fishman et al.*, 1994], it was almost immediately suggested that the source was associated with sprites or other high-altitude (>30 km) phenomena [*Franz et al.*, 1990; *Roussel-Dupré and Gurevich*, 1996; *Inan et al.*, 1996; *Nemiroff et al.*, 1997]. However, in 2003, *Dwyer et al.* [2004a] observed a similar flash of gamma rays on the ground at sea level, apparently emanating from the overhead thunderstorm. This led them to suggest that TGFs originate not from sprites but from thunderstorms deeper in the atmosphere.

[3] In 2005, new TGF observations from the Reuven Ramaty High-Energy Solar Spectroscopic Imager (RHESSI) satellite showed a spectral hardening above 1 MeV [*Smith et al.*, 2005]. *Dwyer and Smith* [2005] performed detailed Monte Carlo calculations and showed that this spectral hardening resulted from the propagation of the gamma rays through a deep layer of atmosphere. Furthermore, they found that the RHESSI gamma-ray spectrum is consistent with bremsstrahlung emission from energetic electrons produced by relativistic runaway electron avalanche (RREA) multiplication [*Gurevich et al.*, 1992] with a source depth in the atmosphere between 130 g/cm^2 and 50 g/cm^2, depending upon the amount of beaming. This corresponds to an altitude range of 15–21 km above sea level, comfortably within the range of thunderstorm heights and much too low for sprites.

[4] In addition, using sferic observations *Cummer et al.* [2005] found that 13 of the RHESSI TGFs were associated with positive polarity lightning discharges, but the charge moment changes of these events were too small to be associated with sprites and were about two orders of magnitude smaller than required by models that assumed that the emission was from high-altitude (>30 km) RREA multiplication.

[5] Not only is a low-altitude source, e.g., <21 km, inconsistent with sprite models of TGFs [*Williams et al.*, 2006], it is also inconsistent with electromagnetic pulse (EMP) models, which produce a very high-altitude source. For example, *Inan and Lehtinen* [2005] proposed a model in which very large and very fast lightning return strokes generate an EMP that, in conjunction with an extensive cosmic-ray air shower, generates runaway electrons above 35 km, contradicting inferred RHESSI source altitudes. For this reason, EMP models will not be considered further in this paper.

[6] One reason that high-altitude models of TGFs were initially favored is that gamma rays are rapidly attenuated in the atmosphere, and so a source low in the atmosphere would require very large fluxes of gamma rays at the source in order to result in the observed fluxes at spacecraft altitudes. Indeed, *Dwyer and Smith* [2005] estimated that the number of runaway electrons at the source must be about 10^{16} for a 21 km source and about 10^{17} for a 15 km source. Exactly how such large numbers of energetic electrons can be produced deep in the atmosphere in short bursts, usually lasting less than a few milliseconds, is a great theoretical challenge. Moreover, since the exact source

[1]Department of Physics and Space Sciences, Florida Institute of Technology, Melbourne, Florida, USA.

0148-0227/08/2007JD009248

location is not known, the ambient conditions that are present at the time of the TGF are also not known, adding to the difficulty of the problem. Nevertheless, it will be shown in this paper that, using BATSE and RHESSI observations, enough information about the source has been established to constrain the possible source mechanisms. In particular, the fluence (photons per unit area) and timing of the TGFs shall be used to rule out the RREA models that have been extensively developed over the last 15 year, which use cosmic rays as the source of the energetic seed particles. It also will be shown that the most likely TGF source mechanisms involve either a recently introduced mechanism called relativistic feedback [*Dwyer*, 2007] or the energetic particle emission from lightning leaders or streamers, similar to the energetic radiation observed on the ground in association with lightning [*Moore et al.*, 2001; *Dwyer et al.*, 2003, 2004b, 2005a] and laboratory sparks [*Dwyer et al.*, 2005b].

2. Cross-Sectional Area of the Source Region

[7] The time structure of individual gamma-ray pulses within BATSE TGFs can be used to determine an upper limit on the dimensions of the source region. This analysis uses the same basic technique often used in astrophysics to estimate the size of distant objects such as quasars. If variations of the intensity are seen with a timescale, T, then the size of the object over which the intensity is significant can be no more than cT where c is the speed of light. If the propagation speed of information is less than the speed of light then the maximum size will be even smaller. The argument is simple: in order for some region to switch states from, for example, low gamma-ray emission to high gamma-ray emission, sufficient time must elapse for the change in state to propagate across the region. For example, if the gamma rays are driven by a change in the electric field, then this change cannot propagate faster than c.

[8] BATSE TGFs are often made up of several fast pulses. *Nemiroff et al.* [1997] analyzed the time structures of these pulses for 13 BATSE TGFs. They found that the variability occurred over a timescale ranging from 26 μs up to 250 μs, with 50 μs being typical. To be conservative, the typical value of 50 μs will be considered here. Nevertheless, BATSE TGF 1433, according to *Nemiroff et al.* [1997], had a minimum timescale of 26 μs. Because 1433 appears to be a typical two peaked BATSE TGF, with a fluence comparable to other BATSE TGFs (see http://www.batse.msfc.nasa.gov/batse/tgf/), any potential mechanism for explaining TGF gamma-ray production should work as well for a source region size less than or equal to that inferred from 1433. For signals traveling at the speed of light, a 50 μs timescale corresponds to a source region size less than 15 km. Alternatively, if signals within the source region propagate via lightning return strokes with $v \sim 10^8$ m/s, this gives a source region size no larger than 5 km. If positive lightning leaders are the source, taking $v \sim 10^7$ m/s as a typical leader speed, then the source region would have a size of at most 500 m. Dart leaders propagating along an existing warm channel typically propagate at $v \sim 10^7$ m/s, which again corresponds to a source size of only 500 m. Finally, using the upper end of the propagation speed of negative stepped leaders, $v \sim 10^6$ m/s, gives just 50 m for the maximum size of the source region, comparable to the length of one step of a negative stepped leader. These estimates of the upper limit on the TGF source region size, which are summarized in Table 1, will be used later in this paper when considering specific source mechanisms.

3. Relativistic Runaway Electron Avalanche Models

[9] The generation of relativistic runaway electron avalanches (RREAs) from cosmic rays has been the most common mechanism used to model TGFs [*Roussel-Dupré and Gurevich*, 1996; *Gurevich and Zybin*, 2001, *Lehtinen et al.*, 1996; *Carlson et al.*, 2007]. The RREA mechanism produces runaway electrons via hard elastic scattering of energetic electrons with atomic electrons, resulting in an avalanche of fast electrons that increases exponentially with distance. The electric field threshold to generate such runaway electron avalanches is $E_{th} = 284$ kV/m $\times$ (n/n_o), where n is the density of air and n_o is the density of air at STP [*Dwyer*, 2003; *Coleman and Dwyer*, 2006]. The RREA mechanism is sometimes erroneously called ''runaway breakdown,'' which is a misnomer, since it is not self-sustaining (i.e., it relies on an external particle source to operate) and thus is not a true electrical breakdown. Because the RREA mechanism depends upon an external source of energetic seed electrons to produce avalanches of runaway electrons, the flux of runaway electrons cannot be calculated without first specifying the flux of the seed population. As a result, RREA models of TGFs are necessarily tied to the source of energetic seed electrons. On the other hand, relativistic runaway electron avalanches produce a unique energy spectrum, nearly independent of the ambient conditions occurring in the source region such as the gas density, electric field strength or the details of the seed population [*Dwyer*, 2004; *Dwyer and Smith*, 2005].

[10] The TGF energy spectrum as measured by RHESSI is consistent with bremsstrahlung emission from relativistic runaway electrons generated by relativistic runaway electron avalanches [*Dwyer and Smith*, 2005]. It is, therefore, reasonable to assume that relativistic runaway electron avalanches play a role in the source of TGFs. Furthermore, the gamma-ray energy spectrum as measured by RHESSI often extends to above 20 MeV [*Smith et al.*, 2005]. This means that the energetic electron spectrum at the source must also extend up to at least this energy.

[11] The avalanche (e-folding) length of relativistic runaway electrons is well fit by the empirical relation,

$$\lambda = \frac{7300kV}{[E - (276kV/m)n/n_o]}, \tag{1}$$

Table 1. Maximum Possible TGF Source Radius[a]

Propagation	Speed, m/s	Maximum Source Radius, m
Speed of light	3×10^8	15,000
Lightning return stroke	1×10^8	5000
Positive lightning leader	1×10^7	500
Lightning dart leader	1×10^7	500
Negative lightning stepped leader	1×10^6	50

[a]The maximum radius is based on a 50 μs variability, for different propagation speeds within the source region.

valid over the range $E = 300–3000$ kV/m $\times$ (n/n_o), where the electric field, E, is measured in kV/m [*Dwyer*, 2003; *Coleman and Dwyer*, 2006]. For a uniform electric field of length λ, the maximum kinetic energy that an electron can gain occurs when the electron traverses the entire length, λ. The maximum kinetic energy is then

$$\Delta K_{\max} = [eE - f_d\ n/n_o]\lambda, \tag{2}$$

where f_d is the average energy loss per unit length owing to interactions with air. Detailed Monte Carlo simulations show that when averaged over the runaway electron distribution function above 1 MeV, f_d has a typical value of 270 keV/m. Therefore, multiplying equations (1) and (2) together gives a maximum energy gain by runaway electrons over one avalanche length of about 7 MeV [*Dwyer*, 2004]. This maximum energy is approximately independent of the gas density and the electric field strength present in the source region. Therefore, because electrons with energies of more than 20 MeV occur in the TGF source region, a minimum of 3 relativistic runaway electron avalanche lengths are likely to be present. This illustrates that at least some RREA multiplication must be going on, which justifies the use of the RREA spectrum when modeling TGFs.

[12] On the other hand, just because relativistic runaway electron avalanches are occurring in the source region of TGFs does not automatically imply that this is the sole mechanism for generating energetic electrons and hence the gamma rays. For example, if we suppose that the TGF source region contains just 3 relativistic runaway electron avalanche lengths and has a cross-sectional area of 100 km^2, then the flux of energetic seed particles injected into the avalanche region would have to be at least 5×10^9 m^{-2} s^{-1} in order to account for the RHESSI TGF observations. That flux of energetic seed particles is about 500,000 times larger than the maximum flux of atmospheric cosmic rays and other sources of energetic background radiation (10^4 m^{-2} s^{-1}). Consequently, there would have to be some other mechanism to increase the flux of energetic electrons by a factor of 500,000 before the modest increase of 20 owing to relativistic runaway electron avalanche multiplication occurs. By increasing the amount of avalanche multiplication and/or the cross-sectional area of the source region it is possible to increase the role of the RREA mechanism. However, as will be shown below, on the basis of the current observations, it is not possible to find a scenario in which RREA acting on external seed particles is the sole mechanism for TGFs. Specifically, it will be shown that constraints placed on the electric field strength and geometric size limit the avalanche growth. However, such limits on the runaway electron production may be circumvented by the feedback mechanisms introduced in the next section.

4. Relativistic Feedback

[13] *Dwyer* [2003, 2007] showed that a positive feedback effect caused by backward propagating runaway positrons and back-scattered x-rays can generate large numbers of energetic seed electrons, allowing the runaway electron discharge to become self-sustaining and no longer requiring an external source of energetic seed particles [see also *Babich et al.*, 2005]. *Dwyer* [2007] referred to this mechanism as relativistic feedback and the state when the discharge becomes self-sustaining as relativistic breakdown. Unlike so-called "runaway breakdown," relativistic breakdown produced by the relativistic feedback mechanism is a true electrical breakdown under the standard use of the term, since the discharge is self-sustaining and results in the collapse of the electric field. *Dwyer* [2007] showed that once relativistic breakdown commences it will discharge the large-scale electric field in less than a millisecond and will result in a flux of runaway electrons up to 10^{13} times larger than from the RREA mechanism alone.

[14] A useful parameter for describing relativistic feedback is the feedback factor, γ, i.e., the average number of secondary runaway electrons, caused by relativistic feedback, per initial runaway electron (see *Dwyer* [2007] for a more detailed discussion). Note that the feedback factor should not be confused with the Lorentz factor, which shares the same symbol and sometimes appears when describing runaway electrons. Instead, the feedback factor is analogous to the second Townsend coefficient for low-energy discharges.

[15] According to *Dwyer* [2007], the feedback factor $\gamma \sim \exp(\xi)/\exp(\xi_o)$, where $\exp(\xi)$ is the runaway electron avalanche multiplication factor; ξ is the number of avalanche lengths; and $\exp(\xi_o)$ and ξ_o are the runaway electron avalanche multiplication factor and the number of avalanche lengths, respectively, that result in a self-sustaining runaway discharge. If τ is the time between successive generations of runaway electrons produced by relativistic feedback, then for $\gamma > 1$ the flux of runaway electrons will increase exponentially with an e-folding time $\tau' \equiv \tau/\ln(\gamma)$. The runaway electron flux at time $t \gg \tau$ after the relativistic feedback begins is

$$F_{re} \approx \begin{cases} S_o \exp(\xi) \exp(t/\tau')/(\gamma - 1), & \gamma > 1 \\ S_o (t/\tau) \exp(\xi), & \gamma = 1\,, \\ S_o \exp(\xi)/(1 - \gamma), & \gamma < 1 \end{cases} \tag{3}$$

where S_o is the flux of external energetic seed particles that run away, e.g., the flux owing to atmospheric cosmic-ray particles and radioactive decays (see section 8 for further details). Because for $\gamma \geq 1$ the discharge becomes self-sustaining, $\gamma = 1$ is the relativistic breakdown threshold.

[16] In comparison to equation (3), the flux of runaway electrons generated by the RREA mechanism acting on an external source of seed particles without feedback is $F_{re} \approx S_o \exp(\xi)$. Therefore, for the case where $\gamma < 1$, relativistic feedback simply serves to increase the flux of runaway electrons by a constant factor of $(1 - \gamma)^{-1}$. In this case, the behavior of the runaway discharge is the same as the RREA mechanism as has been described in a large body of previous work (see *Gurevich and Zybin* [2001] and references therein), albeit with an enhanced flux. In contrast, for the case $\gamma \geq 1$ and especially for $\gamma > 1$, the runaway discharge becomes an electrical breakdown with dramatically different behavior. In this case, unlike the standard RREA mechanism, the peak flux and total number of runaway electrons generated are independent of both the flux of seed particles and the avalanche multiplication factor [*Dwyer*, 2007]. The characteristic timescale of the discharge also decreases by many orders of magnitude.

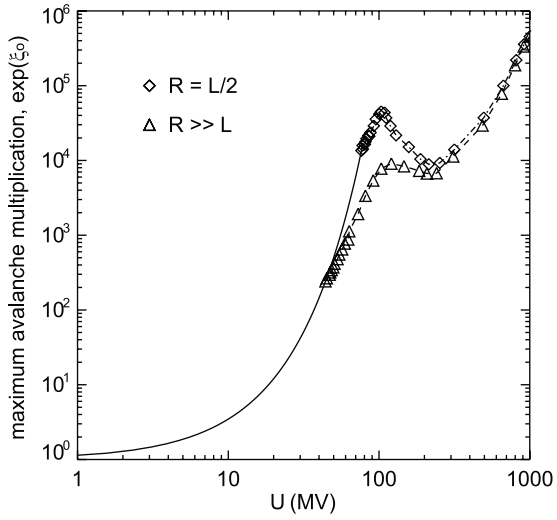

Figure 1. Maximum sustainable relativistic runaway electron avalanche multiplication factor, $\exp(\xi_o)$, versus total potential difference within the avalanche region. The data points (and the dashed and dashed-dotted lines) are the result of Monte Carlo simulations and show the threshold at which the discharge becomes self-sustaining ($\gamma = 1$). The data are calculated for the condition that the lateral radius, R, is much larger than the length of the avalanche region, L, and when it is one half the length. The solid curve on the left side of the plot is given by equation (4).

[17] The avalanche multiplication factor, $\exp(\xi_o)$, that results in $\gamma = 1$ is plotted in Figure 1 against the total potential difference in the avalanche region for a uniform electric field above the runaway electron avalanche threshold and with no external magnetic field. Because the $\gamma = 1$ condition depends upon the width of the avalanche region compared with its length, two extreme cases are considered here: the width of the avalanche region in the simulation equals the length of the region (diamonds and dashed-dotted line) and the width is much larger than the length (triangles and dashed line). The former case is a reasonable approximation of the smallest lateral extent of the avalanche region compared with its length, considering the electrostatic configurations that are likely to be present inside and above thunderstorms. The latter case is most relevant for applications of the RREA mechanism in TGFs, since, as will be discussed below, models in which RREA acts on external seed particles require very large lateral extents of the source region.

[18] Because of the exponential increase in the number of runaway electrons with time, once $\gamma > 1$ the electric field in the avalanche region will be rapidly discharged. As a result, the data plotted in Figure 1 represent an upper limit on the maximum sustainable runaway electron avalanche multiplication factor in air.

[19] In the figure, the data are the result of Monte Carlo simulations. The Monte Carlo, which includes all the detailed physics of the runaway electrons, positrons and energetic photons, is described in depth in the work of *Dwyer* [2007] and references therein and so will not be described here. In addition, the methodology for calculating the data presented in this paper is also described in detail in the work of *Dwyer* [2007], and so will be only summarized here: Relativistic feedback was recorded by keeping track of the electrons and photons that pass through the plane midway between the top and bottom of the avalanche region with a uniform electric field. Many simulations were performed, varying both the length of the avalanche region and the electric field strength, allowing the condition $\gamma = 1$ to be found. In the figure, the peak at $\sim$100 MV is caused by the transition between the x-ray feedback dominated regime, to the left of the peak, and the positron feedback dominated regime to the right. To the left of the data points, the solid curve is not due to relativistic feedback. Instead, it is the limit set by the conventional breakdown field E_b = 3000 kV/m $\times$ (n/n_o). For a uniform electric field, the number of avalanche lengths is $\xi = U/(E\lambda)$, where U is the electric potential difference in the avalanche region. Because $E\lambda$ monotonically decreases with the electric field strength, if we assume that E_b is the maximum large-scale electric field that is likely to occur, then the maximum multiplication factor is

$$\exp(\xi) < \exp\left(\frac{U}{E_b\lambda(E_b)}\right) < \exp\left(\frac{U}{7.3MV}\right), \qquad (4)$$

where $\lambda(E_b)$ is the avalanche length calculated at E_b. The right most inequality in equation (4) was first derived in the work of *Dwyer* [2004] and remains true for nonuniform electric fields and is independent of the air density.

[20] On the basis of Figure 1, it is unlikely that the avalanche multiplication factor can ever exceed about 10^5 for realistic conditions. In Figure 1, the rise to the far right of the plot is caused by positron annihilation as the length of the avalanche region becomes very large. This part of the plot corresponds to electric fields extending over very large distances with very large potentials. For example, in order to exceed 10^5 in the right most part of the plot, the total potential difference would have to be larger than 700 MV and the overall length of the high field region with $E >$ 305 kV/m $\times$ (n/n_o) would have to be longer than 8.5 km. The right most data points correspond to an average electric field of 305 kV/m and a potential difference of 1 GV. Regardless of relativistic feedback, any average electric field less than 300 kV/m would require more than 1 billion volts potential difference in the high field region in order to generate an avalanche multiplication factor greater than 10^5. Such large voltages are not likely to exist in our atmosphere.

[21] As will be shown below, in order for RREA models alone to account for TGFs, very large lateral extents must be assumed. In this case, the $R \gg L$ data in Figure 1 should be used. In addition, it could be argued that potential differences of a few hundred MV are much more likely to occur than 1 GV potentials, and so a limit of $\exp(\xi) < 10^4$ could also be used, albeit with some additional assumptions. For example, if it is assumed that the maximum potential difference inside a thunderstorm is 1 GV, then the largest electrostatic potential difference that could be produced by a lightning discharge in the space above the thunderstorm is about 500 MV, so that for a discharge above the thunderstorm, assuming an approximately electrostatic field, then 2×10^4 is the limit on $\exp(\xi)$.

[22] If relativistic feedback is not taken into account, as was the case for most previous work on the subject, then

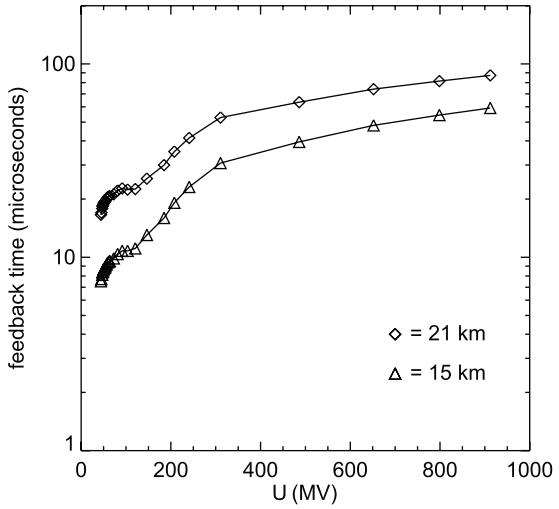

Figure 2. Relativistic feedback time, i.e., the e-folding time for the flux to increase owing to relativistic feedback. The triangles are for a source altitude of 15 km, and the diamonds are for a source altitude of 21 km. This is the timescale required for relativistic feedback to become important.

equation (4) would be the only limit on the avalanche multiplication factor, $\exp(\xi)$, and the solid curve in Figure 1 would continue to rise rapidly as the potential difference increased. To illustrate the dramatic difference that relativistic feedback makes on limiting the avalanche multiplication factor, at $U = 200$ MV, according to equation (4), $\exp(\xi)$ can be as large as $\sim 10^{12}$. However, when relativistic feedback is included, $\exp(\xi) < 10^4$ for the $R \gg L$ case, 8 orders of magnitude lower than when relativistic feedback is not considered. Note that limiting the avalanche multiplication factor does not mean that fewer runaway electrons are being produced. Indeed, as can be seen in equation (3), including relativistic feedback can result in many orders of magnitude more runaway electrons by increasing the number of avalanches. Therefore, many previous RREA models, which do not include effects of relativistic feedback, grossly overestimate the avalanche multiplication, sometimes affecting the validity of the results.

[23] The timescale required for relativistic feedback to become important is plotted in Figure 2 for two source altitudes (for R $\gg$ L). This time, τ', as defined above, is the time needed for the flux of runaway electrons created by relativistic feedback to increase by one e-folding. For this figure, the curves plotted assume that the $\gamma = 1$ condition is exceeded by 1 avalanche length, i.e., $\gamma = e^1$. In other words, we add one avalanche length to a breakdown that is just barely self-sustaining. For models in which RREA acts on external sources of seed particles alone, in order to have an avalanche multiplication factor greater than the limit shown in Figure 1, a TGF described by these models could not have a duration longer than shown in Figure 2. Because for all cases, the feedback time shown in Figure 2 is less than the duration of TGFs, the upper limit on the avalanche multiplication factor in Figure 1 fully applies to TGFs.

[24] To augment the detailed Monte Carlo calculations, *Dwyer* [2007] developed a simple model of the discharge of the electric field owing to relativistic feedback. It was found that the electric field at the end of the avalanche region was reduced by 1/e in the time

$$t_{dis} = \tau' \ln\left(\frac{(\gamma - 1)\varepsilon_o}{l_e \mu' e S_o \tau'^2 \exp(\xi)}\right), \tag{5}$$

referred to as the discharge time. Here $\mu' = \frac{\mu_e}{\left(1 + \frac{\tau'}{\tau_a}\right)} + \frac{\mu_-}{\left(1 + \frac{\tau_a}{\tau'}\right)} + \mu_+$, where τ_a is the attachment time of free low-energy electrons and μ_e, μ_- and μ_+ are the mobilities of the electrons and ions (note: this notation has changed from *Dwyer* [2007]). In equation (5), l_e is the ionization per unit length caused by the runaway electrons (see section 8 for further details), and all other symbols are either defined above or have their usual meaning. Equation (5) is plotted for a TGF source at 15 km and 21 km in Figure 3, using results of Monte Carlo calculations for $\exp(\xi)$ and τ' as presented in Figures 1 and 2 (for R = L$\neq$2). For the figure, the value $S_o \sim 10000\ \mathrm{m}^{-2}\ \mathrm{s}^{-1}$ is used [*Hillas*, 1972], the maximum that is likely to occur in our atmosphere and $\gamma = e^1$. The values chosen for the other parameters in equation (5) will be discussed below in section 8. Note this figure differs slightly from *Dwyer* [2007, Figure 9], which was calculated for a source at sea level. The discharge time plotted in Figure 3 can be viewed as the approximate duration of a TGF predicted by this simple relativistic feedback model. Note that this time is in the exact range of TGF durations observed by BATSE and RHESSI.

[25] The fluence (electrons/m^2) of runaway electrons generated by relativistic feedback is given by *Dwyer* [2007, equation (39)]

$$Fluence = \frac{\varepsilon_o}{l_e \mu' e \tau'} \tag{6}$$

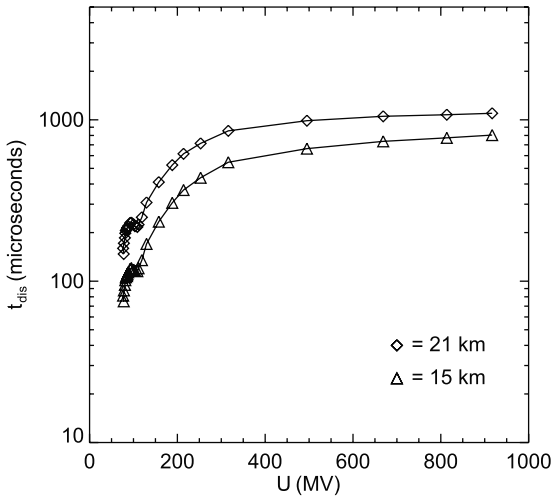

Figure 3. Discharge time owing to relativistic feedback. The triangles are for a source altitude of 15 km, and the diamonds are for a source altitude of 21 km. This is the time for relativistic feedback to reduce the electric field at the end of the avalanche region by 1/e.

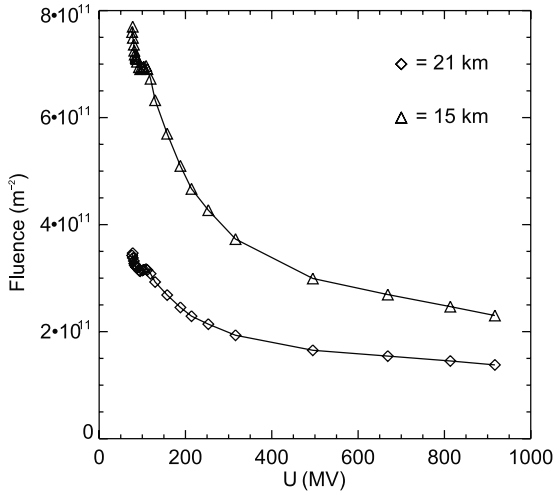

Figure 4. Fluence of runaway electrons (electrons/m^2) owing to the relativistic feedback mechanism, assuming that the production of runaway electrons terminates at time, t_{dis}. The triangles are for a source altitude of 15 km, and the diamonds are for a source altitude of 21 km.

and is plotted in Figure 4 (for R = L$\neq$2). Note that equation (6) does not depend explicitly on the amount of avalanche multiplication. Because the fluence multiplied by the source area must equal the number of runaway electrons at the source, equation (5) along with the number of runaway electrons at the source inferred by the RHESSI data give an estimate of the TGF source radius. This source radius is plotted in Figure 5 for source altitudes of 15 km and 21 km. As can be seen, the source radii required by relativistic feedback are quite modest and are on the order of only 100 m, which is very reasonable for the highest field region inside thunderstorms. These radii are also consistent with the upper limit on the size of the source region discussed in section 2 above, with the exception of the case of negative stepped leaders, which is probably not applicable to the present discussion.

[26] Finally, because relativistic feedback is very efficient at discharging electric fields, even for the case $\gamma < 1$, the question naturally arises: how does a thunderstorm manage to develop a region with an electric field large enough to produce a self-sustaining discharge (i.e., $\gamma > 1$)? *Dwyer* [2005] proposed such a mechanism, showing how a discharge produced by runaway electrons could rapidly ramp up the electric field in some parts of the avalanche region, resulting in a self-sustaining discharge and possibly lightning initiation. Alternatively, a lightning discharge could potentially produce local field enhancements that result in a self-sustaining discharge.

5. RREA Models Involving Extensive Cosmic-Ray Air Showers

[27] Extensive cosmic-ray air showers are often invoked, along with the RREA mechanism, to explain a wide range of atmospheric phenomena, including lightning initiation, narrow bipolar pulses (NBPs) and TGFs [*Gurevich and Zybin*, 2001, 2005]. The reason is that extensive air showers can impulsively inject very large numbers of energetic seed particles into the high field region where runaway electron avalanches are occurring. The resulting avalanche multiplication can in turn produce even larger numbers of runaway electrons. However, despite the popularity of extensive cosmic-ray air showers, there are several lines of evidence that strongly suggest that they do not play a major role in TGF production.

[28] For extensive cosmic-ray air showers, the number of energetic seed particles, N_e, injected into the TGF source region depends upon the energy of the primary cosmic ray. In particular, the number of secondary energetic particles at shower maximum (mostly electrons and positrons) is described by the approximate relation

$$N_{EAS} \sim 5 \times 10^{-2} E_o^{1.1}, \tag{7}$$

where E_o is the total energy of the cosmic-ray primary measured in GeV [*Gaisser*, 1990]. For example, N_{EAS} is $\sim 2 \times 10^5$ for a primary energy of 10^{15} eV.

[29] Using the upper limit on the avalanche multiplication factor, $\exp(\xi) < 10^5$, discussed above, in order to generate 10^{16} runaway electrons at the TGF source, the minimum required, the air shower would have to inject at least 10^{11} particles. From equation (7), this would correspond to a primary cosmic ray with energy above 10^{20} eV, near the very maximum energy ever observed. The flux of such ultra-high-energy cosmic rays is extremely small, and is only about 1 km^{-2} sr^{-1} century^{-1} [*Longair*, 1992].

[30] After taking into account the gamma-ray propagation through the atmosphere, the runaway electrons creating the TGF are produced over a timescale ranging from about 0.1 to 10 ms. These relatively long timescales are very difficult to explain when modeling TGFs using extensive cosmic-ray air showers. Specifically, air showers propagate at the speed of light, and most of the avalanche multiplication results from seed particle injection in the first few avalanche lengths. Below 21 km, for fields above 300 kV/m $\times$ (n/n_o), this means that an extensive air shower should produce

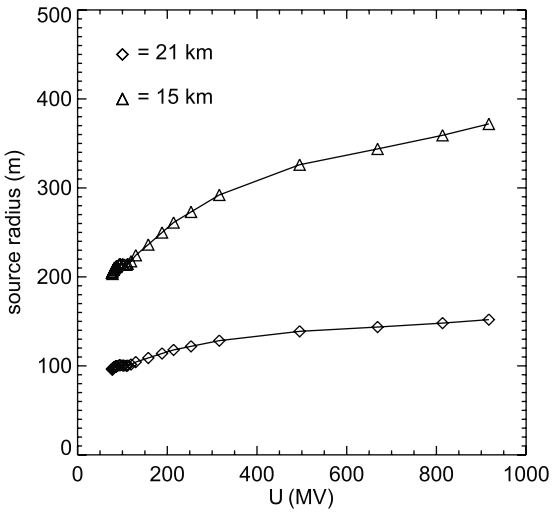

Figure 5. TGF source radius that would be required to produce 1×10^{17} runaway electrons at 15 km (triangles) and 1×10^{16} runaway electrons at 21 km (diamonds) given the fluences of runaway electrons shown in Figure 4.

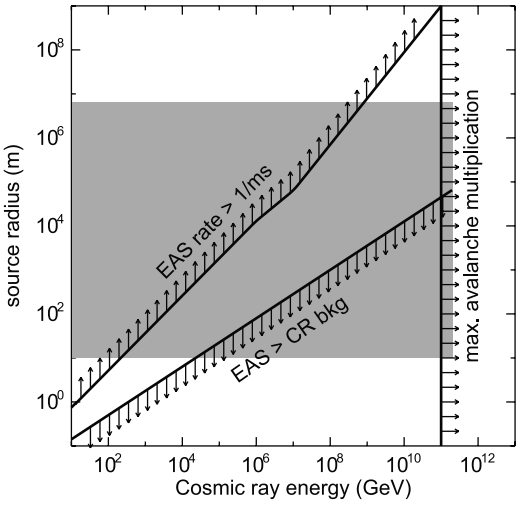

Figure 6. Constraints on extensive cosmic-ray air showers as a source of seed electrons for the RREA mechanism for TGFs. The plot shows the required TGF source radius versus primary cosmic-ray energy. The arrows show the side of each curve that is allowed. The vertical line labeled "max. avalanche multiplication" is the required cosmic-ray primary energy resulting from the maximum avalanche multiplication factor shown in Figure 1. The upper curve labeled "EAS rate > 1/ms" is the requirement of producing multiple peaks within a TGF. The lower curve labeled "EAS > CR bkg" is the requirement that the extensive air shower produces more seed particles than the ambient cosmic-ray background. The grey shade region shows the range over which extensive air shows could be considered.

a gamma-ray pulse lasting on the order of 10 μs, 10 times too fast for even the shortest TGFs.

[31] An even bigger difficulty is the fact that BATSE and RHESSI frequently observed multiple pulses within a TGF, all of comparable size. This indicates that the frequency of TGFs cannot be tied to the coincidence rate between the air showers and events associated with the thunderstorm. For example, suppose that owing to some unknown process inside or above the thunderstorm, the electric field rapidly increases to above the runaway avalanche threshold so that many runaway avalanche lengths occur. Then, a short time later the field rapidly discharges. Because the TGFs are observed to often last several milliseconds, the field must remain strong for at least this time. Assume for a moment that a TGF is the result of a coincidence between an extensive air shower and the occurrence of this high field region. Because multiple pulses are often seen in TGFs, recalling the timing discussion above, presumably each one of these pulses should be identified with a separate air shower. Therefore, the occurrence rate of these air showers must be at least 1/ms. One conclusion is that every time that the thunderstorm produces a high electric field capable of making a TGF, there would be a high probability that an air shower with sufficient energy occurred within that time period. This occurrence rate of extensive air showers can be used to estimate the size of the source region. The integral flux of extensive air showers in the range 10^{10}–10^{20} eV (assuming an approximately isotropic arrival distribution from above) is given roughly by

$$\begin{array}{ll} I(>E_o) = 3\times 10^4 E_o^{-1.7} m^{-2} s^{-1} & 10GeV < E_o < 3\times 10^6 GeV \\ I(>E_o) = 4\times 10^7 E_o^{-2.1} m^{-2} s^{-1} & E_o > 3\times 10^6 GeV \end{array}, \tag{8}$$

where E_o is the energy of the cosmic-ray primary particle in GeV [*Berezinskii et al.*, 1990].

[32] Requiring one air shower per millisecond implies that

$$I\,A > 1000 s^{-1}, \tag{9}$$

where A is the cross-sectional area of the source region. The lower limit on the source radius, determined by equations (8) and (9), is plotted in Figure 6. In the figure, the arrows indicate which side of the line is allowed. For this case, only the space above the upper diagonal line is permitted. Also shown is the minimum required cosmic-ray energy of 10^{20} eV determined by relativistic feedback (vertical line). The feedback limit and the limit from equations (8) and (9), when combined, require that the area of the source region to be several orders of magnitude larger than the entire surface area of the earth. In contrast, the physical range of possible extensive air showers and possible TGF source regions is shown in Figure 6 as the gray shaded region. The top of the gray region is limited (extremely conservatively) by the size of the earth. The bottom is a reasonable lower limit based on the likely lateral size of a high field region considering that the length of the high field region must be at least 20 m (see equation (1) and the discussion above). In addition, extensive air showers can themselves have considerable lateral extent. The right side of the gray region is determined by the highest-energy extensive air shower ever measured: a few times 10^{20} eV. There are also theoretical reasons, on the basis of the propagation of the cosmic rays through intergalactic space, to expect that the spectrum does not extend much higher in energy.

[33] A final problem is that because the energy spectrum of cosmic rays falls off so rapidly with primary cosmic-ray energy, for every air shower above a given energy, there will be many more with lower energies. For example, for every cosmic ray above 10^{16} eV, there will be more than 50 with energies above 10^{15} eV and so forth. The rate of all cosmic-ray secondary particles is about S_o = 10000 m^{-2} s^{-1} for altitudes where shower maximum usually occurs ($\sim$100 g/cm^2) [*Hillas*, 1972]. For a Δt = 1 ms time interval, a source region with a cross-sectional area A will have

$$N_{cr} \cong 10 \frac{particles}{m^2} A \tag{10}$$

energetic seed particles. If cosmic-ray air showers are the source of TGFs, then the number of secondary particles injected by a single extensive air shower (e.g., equation (7)) must be at least as large as the number injected by the steady state cosmic-ray background in 1 ms (equation (10)). This means that $N_{EAS} > N_{\rm cr}$. Plugging equations (7) and (10) into this inequality gives

$$A < 5\times 10^{-3} E_o^{1.1}, \tag{11}$$

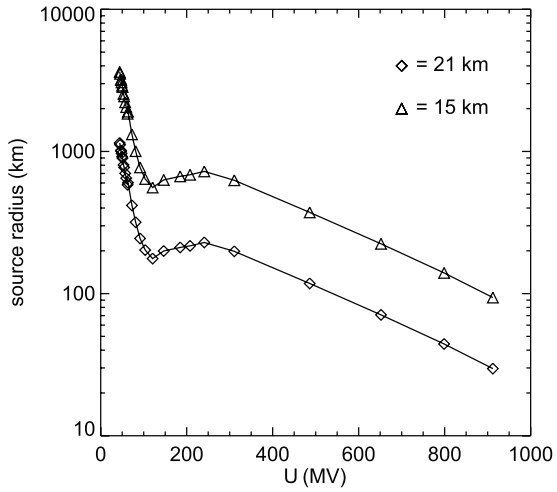

Figure 7. TGF source radius that would be required to produce 1×10^{17} runaway electrons at 15 km (triangles) and 1×10^{16} runaway electrons at 21 km (diamonds) by the RREA mechanism acting on the cosmic-ray background.

where E_o is measured in GeV and A is in m^2. This inequality is plotted in Figure 6 (bottom diagonal line). As can be seen in the figure, because the upper limit set by equation (11) is much below the lower limit set by equations (8) and (9), there exists no source region that simultaneously satisfies the necessary constraints set by TGF observations if extensive air showers provide the seed runaway electrons. In summary, it is extremely improbable that extensive air showers and the RREA mechanism play any significant role in TGFs.

6. RREA Models Involving the Steady State Background Radiation

[34] If extensive air showers are not involved in TGFs, then in order for the RREA mechanism alone to explain TGFs we must search for an alternate source of the energetic seed particles. The remaining candidate is the steady state background radiation produced mainly by cosmic rays (of all energies) with some possible contribution from radioactive decays, such as from radon in the atmosphere.

[35] Consider the total number of runaway electrons that can be produced by RREA models acting on atmospheric cosmic rays. At sea level the vertical flux of atmospheric cosmic rays is about 200 m^{-2} s^{-1}. At thunderstorm altitudes this number peaks at about 10^4 m^{-2} s^{-1} [*Hillas*, 1972]. Integrating the largest atmospheric cosmic-ray flux over the typical TGF duration of 1 ms gives 10 m^{-2} (equation (10)). Multiplying this by the largest possible avalanche multiplication factor plotted in Figure 1 and requiring that 10^{16} runaway electrons be produced for a 21 km source altitude, and 10^{17} runaway electrons be produced for a 15 km source altitude, gives the minimum source radius plotted in Figure 7. As can be seen, the source radius must be at least 30 km if the source altitude is at 21 km and the source radius must be at least 100 km if the source altitude is 15 km. However, both these source radii are for the extreme case of nearly 1 billion volts potential difference in the high field region. A more reasonable potential difference, especially above the thunderstorm, of 500 MV requires a source radii of at least 100 km and 400 km for 21 km and 15 km source altitudes, respectively. In addition to contradicting the maximum size of the TGF source region discussed in section 2, these numbers seem unphysically large for a region that has an elevated electric field >300 kV/m $\times$ (n/n_o).

[36] Because the timescale for relativistic feedback to occur is usually a few microseconds to a few tens of microseconds (see Figure 2), any proposed mechanism that rapidly ramps up the electric field so that a self-sustaining discharge occurs will also produce so much feedback over a 1 millisecond timescale that the cosmic-ray source will become completely negligible compared to the relativistic feedback mechanism. Therefore, regardless of the exact mechanism for producing the large electric fields, RREA models acting on external sources of seed particles appear to be very unlikely for explaining TGFs owing to the very large size of the source region that such models would require.

7. High-Field Runaway Electron Mechanism

[37] Although relativistic feedback appears to be able to explain many features of TGFs, in this section an alternative mechanism will be discussed: runaway electron production in the high electric fields associated with lightning leaders or steamers.

[38] X-ray emission has been observed on the ground from natural, negative cloud-to-ground lightning, rocket-triggered lightning and long laboratory sparks in air. The x-ray emission is seen to occur in association with the stepped leader formation in natural lightning [*Dwyer et al.*, 2005a] and during the dart leader phase in triggered lightning [*Dwyer et al.*, 2003, 2004b], with possibly some contribution from the beginning of the return stroke. X-rays have also been observed from both positive and negative rod-to-ground plane sparks in air at STP, generated by a 1.5 MV Marx generator, with gap lengths ranging from 0.1 m up to 1.5 m [*Dwyer et al.*, 2005b]. The x-ray emission from laboratory sparks appeared to be very similar to the emission observed from both natural and triggered lightning and so probably shares the same runaway electron production mechanism.

[39] *Dwyer* [2004] showed that the energy spectrum and intensity of x-ray emission from lightning is not consistent with the RREA mechanism and suggested that instead the so-called cold runaway electron mechanism was taking place in the strong electric fields that may occur at either the leader tips or the streamer heads. For the cold runaway electron mechanism, when the electric field exceeds the critical field, $E_c \sim 30$ MV/m $\times$ (n/n_o), about ten times larger than the breakdown field, free thermal electrons may gain sufficient energy to run away [*Gurevich*, 1961; *Moss et al.*, 2006]. As a result, no additional source of energetic seed electrons is required.

[40] Because the exact mechanism for generating runaway electrons and the accompanying x-rays in association with lightning leaders and laboratory sparks is still under debate [*Gurevich et al.*, 2007], the mechanism for producing runaway electrons during lightning and laboratory sparks shall be referred to as "high-field runaway electron production."

[41] When lightning leaders are propagating in strong electric fields inside thunderstorms, it is not unreasonable that they would be producing energetic seed electrons as they do near the ground. In fact, for leaders inside thunderstorms, since the ambient large-scale electric field may be much larger than near the ground, even if the leaders emit the same flux of energetic seed electrons, these electrons could undergo more avalanche multiplication via the RREA mechanism. In addition, leaders propagating in a region with a stronger electric field may also generate more seed electrons, since the cold runaway process is sensitive to the ambient electric field. Alternatively, a large-scale streamer such as occurs in association with sprites could in principle also produce large enough electric fields at its head that cold runaway could be occurring. As with the lightning leader emission, the runaway electrons could then accelerate to relativistic energies, either in a large-scale ambient electric field or the electric field produced by the streamer itself.

[42] Estimating the average number of seed electrons injected by lightning leaders is difficult. *Dwyer et al.* [2004b] estimated that for negative dart leaders from rocket-triggered lightning the number of x-rays generated when the leader was within a few hundred meters of the ground was probably on the order of 10^9. It is not possible to directly calculate the number of energetic electrons that produced these x-rays, since the distance that the electrons propagated is not known. The mean free path of a 250 keV electron (the maximum energy estimated by *Dwyer et al.* [2004b] for triggered lightning dart leaders) for producing a >30 keV x-ray via bremsstrahlung is about 200 m. Considering that the electric field produced by the dart leader falls off over approximately 10 m [*Miki et al.*, 2002; *Jordan et al.*, 1997], suggests that there are about 10^{10} runaway electrons produced by the dart leader in the last 100 m from the ground. Because we are interested in the number of runaway electrons injected into the first avalanche length ($\lambda \sim 100$ m) where additional RREA multiplication can occur, considering only runaway electrons produced over 100 m is reasonable for TGFs. Therefore, if the number of energetic seed electrons were of this order inside the thunderstorm, then assuming the maximum avalanche multiplication factor possible without feedback, only 10 such leaders would be required at 21 km and 100 such leaders at 15 km altitude.

[43] Using the return stroke speed of 10^8 m/s as the characteristic speed that information in the source region propagates gives an upper limit on the radius of the source region of 5 km (Table 1). One such scenario might be a return stroke transferring negative charge to existing negative stepped leaders within the thunderstorm, briefly intensifying the runaway electron production by the leaders. Such a source region would be about 100 times larger than the area at the International Center for Lightning Research and Testing (ICLRT) at Camp Blanding, FL, which is covered by the Thunderstorm Energetic Radiation Array (TERA) currently consisting of 24 x-ray measuring stations. This implies that an event similar to a TGF source at 15 km, seen near the ground, would only need to produce roughly the same x-ray emission over the ICLRT site than is currently observed from triggered lightning. Indeed, such large x-ray events are also frequently observed during natural lightning [*Dwyer et al.*, 2005a].

8. Current and Charge Moment Changes Produced by TGFs

[44] If the source of TGFs is located between 21 and 15 km and produces 10^{16} to 10^{17} runaway electrons, respectively, then regardless of the source mechanism such large numbers of runaway electrons should produce measurable currents and charge moment changes, even if no lightning is associated with the event. In this section, a simple model is used to estimate the values of these current and charge moment changes. This model will follow closely the simple model presented in the work of *Dwyer* [2007]. However, in this model, no specific mechanism for producing the runaway electrons will be assumed. Furthermore, it will not be assumed that the discharge resulting from the runaway electrons is what necessarily terminates the TGF.

[45] Relativistic runaway electrons have an average energy of about 7 MeV, independent of the details of the acceleration region, e.g., independent of the electric field and the gas density. These electrons are nearly minimum ionizing, losing energy in air at a constant rate of about 2.7×10^5 eV/m $\times$ (n/n_o). It is well known that the average energy required to ionize an air atom by energetic particles is 34 eV [*Sauli*, 1977]. This gives $l_e = 8000\ \mathrm{m}^{-1} \times (n/n_o)$ electron-ion pairs per meter per runaway electron. When strong electric fields are present and when the correct energy distribution of runaway electrons is considered, this number will increase slightly. Monte Carlo simulations show that the electron-ion pairs per meter per runaway electron is typically $l_e \sim 9000\ \mathrm{m}^{-1} \times (n/n_o)$.

[46] The low-energy electrons produced by ionization attach to oxygen and water vapor very quickly to form negative ions. As a result, there will be $9000 \times (n/n_o)$ ion pairs per meter per runaway electron. These negative ions, along with the positive ions produced by the ionization, will then drift in the ambient electric field. While drifting, the ions can become attached to cloud droplets or cloud ice crystals. However, using typical water and ice contents of clouds, it is found that the ions will drift several meters before sticking to droplets or ice crystals [*Chiu*, 1978].

[47] The drift speed of low-energy electrons and ions is given by $v = \mu E$, where μ is the mobility of the species. The mobility scales as (n_o/n), where n is the density of air, and n_o is the density of air at STP. At STP, the mobility for low-energy electrons is $9.4 \times 10^{-2}\ \mathrm{m^2\ V^{-1}\ s^{-1}}$, for the positive ions is $1.4 \times 10^{-4}\ \mathrm{m^2\ V^{-1}\ s^{-1}}$ and for the negative ions is $1.9 \times 10^{-4}\ \mathrm{m^2\ V^{-1}\ s^{-1}}$. As an example, at the runaway breakdown threshold field, $E_{th} = 2.84 \times 10^5$ V/m $\times$ (n/n_o), this gives an average drift speed of about 50 m/s for the ions.

[48] For a flux, F_{re}, of runaway electrons moving though a region with electric field strength, E, the electric current density is given by

$$J = e\left(n_e\mu_e + n_-\mu_- + n_+\mu_+\right)E + eF_{re}, \tag{12}$$

where n_e is the number density of the free low-energy electrons produced by ionization of the gas; n_+ is the number of positive ions and n_- is the number of negative ions produced when the electrons attach to oxygen and

water molecules. The number densities are given by the following equations

$$\frac{dn_e}{dt} = l_e F_{re} - \frac{n_e}{\tau_a} \tag{13}$$

$$\frac{dn_-}{dt} = \frac{n_e}{\tau_a} \tag{14}$$

$$\frac{dn_+}{dt} = l_e F_{re}, \tag{15}$$

where τ_a is the attachment time of free low-energy electrons. τ_a is a rather complicated function of electric field strengths, gas density and composition. For air at STP, $\tau_a \sim 10^{-8}$ s and for the altitude ranges and electric field strengths under consideration here scales approximately with (n_o/n). For the altitude range of 15–21 km, $\tau_a \sim 10^{-7}$ s.

[49] Because the timescale of TGFs is on the order of 1 millisecond, which is much longer than the attachment time, τ_a, if we consider the steady state case for which $t \gg \tau_a$, equation (13) has the solution

$$n_e = \tau_a l_e F_{re}. \tag{16}$$

As a result, the ratio of the current from the slow electrons to that of the fast runaway electrons is

$$\frac{J_e}{J_{re}} = \tau_a l_e \mu_e E. \tag{17}$$

This ratio is approximately independent of altitude and has a value of 2.5–25, depending upon the electric field. Therefore, for TGFs, the current from the runaway electrons themselves is less than that from the slow, low-energy electrons.

[50] Integrating equations (14) and (15) for an approximately constant runaway electron flux that is switched on at $t = 0$ gives

$$n_- = n_+ = t l_e F_{re}, \tag{18}$$

where t is the time since the start of the TGF. The ratio of the current from the drifting ions to the slow electrons is therefore

$$\frac{J_i}{J_e} = \left(\frac{t}{\tau_a}\right)\frac{(\mu_- + \mu_+)}{\mu_e}. \tag{19}$$

[51] For TGFs, the current from the ions will dominate over both that of the low-energy electrons and the runaway electrons for $t > 30$ μs in the altitude range 15–21 km. Because 30 μs is much shorter than the duration of all TGFs, this implies that the drifting ions will completely dominate the electrical current produced by a TGF discharge. Note that in this paper, the current from any lightning channels associated with the TGFs is not being considered.

[52] Let N_{re} be the total number of runaway electrons produced by the TGF and let R be the lateral radius of the source region, assuming a vertically downward electric field. Then, the runaway electrons will produce

$$n_i = \frac{N_{re} l_e}{\pi R^2} \tag{20}$$

ion pairs per m^3 at the end of the avalanche region. The positive and negative ions produce an electrical current density of

$$J = \frac{e N_{re} l_e (\mu_- + \mu_+) E}{\pi R^2}. \tag{21}$$

For a plane geometry, the change in the electric field at the end of the avalanche region is

$$\frac{dE}{dt} = -\frac{J}{\varepsilon_o}. \tag{22}$$

Plugging in equation (21) into equation (22) gives an e-folding time for discharging the field of

$$\tau_d = \frac{\varepsilon_o \pi R^2}{e N_{re} l_e (\mu_- + \mu_+)}, \tag{23}$$

assuming that the electric field is reduced owing to the current produced by the TGF and not some other mechanism.

[53] Note the ionization per unit length and the mobility have opposite dependencies on the gas density, so the sea level values can be used in equation (23) for τ_d. Since the current density is proportional to the electric field, the current will also have this τ_d as its e-folding decay time. Plugging in the numbers into the equations above gives $\tau_d = (6 \times 10^{-9}\ \mathrm{s/m^2}) \times R^2$ for a source at 21 km and $\tau_d = (6 \times 10^{-10}\ \mathrm{s/m^2}) \times R^2$ at 15 km. In other words, the decay time in the current can be used to constrain the size of the source region.

[54] In addition, the total charge moment that is produced by the collapse of the electric field is given by

$$M = \varepsilon_o E \lambda \pi R^2, \tag{24}$$

where λ is the runaway avalanche length, with $\lambda \sim 100$ m being a typical number. A basic property of runaway electron avalanches is $E\lambda > 7.3 \times 10^6$ V for all electric fields and densities. Therefore,

$$M > (7.3 \times 10^6 V)\varepsilon_o \pi R^2 = (2 \times 10^{-4} C/m) \times R^2. \tag{25}$$

Measuring the total charge moment then gives an upper bound on the source radius. Combining equations (23) and (25) give the relationship between the total change in the electric dipole moment and the timescale over which the change occurs:

$$M > (7.3 \times 10^6 V) e N_{re} l_e (\mu_- + \mu_+) \tau_d = \begin{cases} (35 C\,\mathrm{km/s}) \times \tau_d & 21\,\mathrm{km} \\ (350 C\,\mathrm{km/s}) \times \tau_d & 15\,\mathrm{km} \end{cases}. \tag{26}$$

[55] In equation (26) and in equations (27) and (28) below the values for N_{re} inferred from RHESSI observations are used in order to give numerical estimates. The combination of observational constraints on M and τ_d should allow additional information such as the number of runaway electrons to be determined. Finally, the total peak current from the TGF ions (not the lightning) is

$$I = J\pi R^2 = eN_{re}l_e(\mu_- + \mu_+)E > eN_{re}l_e(\mu_- + \mu_+)E_{th} \approx \begin{cases} 0.1\ kA & 21\ \text{km} \\ 2\ kA & 15\ \text{km} \end{cases}, \quad (27)$$

where the lower limit on the electric field E_{th} in the avalanche region is used. In addition, the total current should decay with the characteristic time, τ_d.

[56] Multiplying the peak current by the avalanche length gives the peak current moment:

$$I\lambda = eN_{re}l_e(\mu_- + \mu_+)E\lambda > 7.3 \times 10^6 eN_{re}l_e(\mu_- + \mu_+) \approx \begin{cases} 35\ A\ \text{km} & 21\ \text{km} \\ 350\ A\ \text{km} & 15\ \text{km} \end{cases}, \quad (28)$$

which depends upon the number of runaway electrons but has no other altitude dependence. Note that both the peak current and the peak current moment are independent of the source radius. Current measurements, therefore, could be used to constrain N_{re}, the number of runaway electrons at the source.

[57] Although the currents and charge moments are small, they should be observable with existing instrumentation for measuring sferics if the TGF is sufficiently close to the sensor (S. Cummer, private communication, 2007). Especially important would be the observation of TGFs that precede the lightning pulse by some time, so that the current and charge moment changes from the TGF could be separated from that of the lightning. Such observation could place important constraints on characteristics of the TGF source, such as the lateral extent of the source region and number of runaway electrons, which would in turn allow the flux of runaway electrons (number per unit area per second) at the source to be inferred. Finding the flux at the source region would provide a powerful way to discriminate between the different source mechanisms.

9. Summary

[58] The key results of this paper are summarized as follows:

[59] 1. Relativistic runaway electron avalanches (RREAs) acting on an external source of seed particles is insufficient to account for TGF fluxes because they require either unrealistically large lateral sizes or unrealistically large seed fluxes or unrealistically large avalanche multiplication factors.

[60] 2. Extensive cosmic-ray air showers do not play a major role in TGFs, on the basis of observed time structures and fluences of TGFs, the energy spectrum of extensive air showers, the resulting numbers of atmospheric cosmic-ray particles, and the maximum avalanche multiplication factor determined by relativistic feedback.

[61] 3. The relativistic feedback mechanism appears to provide a good explanation of the observed properties of TGFs. It can naturally explain the duration of TGFs and can generate the required number of runaway electrons in a realistic source region measuring just a few hundred meters across.

[62] 4. Runaway electron production in high electric fields, such as occurs in association with natural, triggered lightning and laboratory sparks is a viable alternative to the relativistic feedback mechanism.

[63] 5. The pulse shapes of the BATSE TGFs help constrain the lateral radius of the source region and are useful for constraining the possible source mechanisms, including what lightning processes (if any) could potentially be involved.

[64] 6. Basic properties of the current and charge moment changes have been inferred, which can be compared with sferics data to constrain further such properties as the size of the source region and the number of runaway electrons.

[65] **Acknowledgments.** This work was supported by the NSF grant ATM 0607885.

References

Babich, L. P., E. N. Donskoy, I. M. Kutsyk, and R. A. Roussel-Dupré (2005), The feedback mechanism of runaway air breakdown, *Geophys. Res. Lett.*, *32*, L09809, doi:10.1029/2004GL021744.

Berezinskii, V. S., et al. (1990), *Astrophysics of Cosmic Rays*, Elsevier, New York.

Carlson, B. E., N. G. Lehtinen, and U. S. Inan (2007), Constraints on terrestrial gamma ray flash production from satellite observation, *Geophys. Res. Lett.*, *34*, L08809, doi:10.1029/2006GL029229.

Chiu, C.-S. (1978), Numerical study of cloud electrification in axisymmetric, time-dependent cloud model, *J. Geophys. Res.*, *83*, 5025–5049.

Coleman, L. M., and J. R. Dwyer (2006), Propagation speed of runaway electron avalanches, *Geophys. Res. Lett.*, *33*, L11810, doi:10.1029/2006GL025863.

Cummer, S. A., Y. Zhai, W. Hu, D. M. Smith, L. I. Lopez, and M. A. Stanley (2005), Measurements and implications of the relationship between lightning and terrestrial gamma ray flashes, *Geophys. Res. Lett.*, *32*, L08811, doi:10.1029/2005GL022778.

Dwyer, J. R. (2003), A fundamental limit on electric fields in air, *Geophys. Res. Lett.*, *30*(20), 2055, doi:10.1029/2003GL017781.

Dwyer, J. R. (2004), Implications of x-ray emission from lightning, *Geophys. Res. Lett.*, *31*, L12102, doi:10.1029/2004GL019795.

Dwyer, J. R. (2005), The initiation of lightning by runaway air breakdown, *Geophys. Res. Lett.*, *32*, L20808, doi:10.1029/2005GL023975.

Dwyer, J. R. (2007), Relativistic breakdown in planetary atmospheres, *Phys. Plasmas*, *14*, doi:042901-042901-17.

Dwyer, J. R., and D. M. Smith (2005), A comparison between Monte Carlo simulations of runaway breakdown and terrestrial gamma-ray flash observations, *Geophys. Res. Lett.*, *32*, L22804, doi:10.1029/2005GL023848.

Dwyer, J. R., et al. (2003), Energetic radiation produced during rocket-triggered lightning, *Science*, *299*, 694.

Dwyer, J. R., et al. (2004a), A ground level gamma-ray burst observed in association with rocket-triggered lightning, *Geophys. Res. Lett.*, *31*, L05119, doi:10.1029/2003GL018771.

Dwyer, J. R., et al. (2004b), Measurements of x-ray emission from rocket-triggered lightning, *Geophys. Res. Lett.*, *31*, L05118, doi:10.1029/2003GL018770.

Dwyer, J. R., et al. (2005a), X-ray bursts associated with leader steps in cloud-to-ground lightning, *Geophys. Res. Lett.*, *32*, L01803, doi:10.1029/2004GL021782.

Dwyer, J. R., H. K. Rassoul, Z. Saleh, M. A. Uman, J. Jerauld, and J. A. Plumer (2005b), X-ray bursts produced by laboratory sparks in air, *Geophys. Res. Lett.*, *32*, L20809, doi:10.1029/2005GL024027.

Fishman, G. J., et al. (1994), Discovery of intense gamma-ray flashes of atmospheric origin, *Science*, *264*, 1313–1316.

Franz, R. C., R. J. Nemzek, and J. R. Winckler (1990), Television image of a large upward electrical discharge above a thunderstorm system, *Science*, *249*, 48.

Gaisser, T. (1990), *Cosmic Rays and Particle Physics*, Cambridge Univ. Press, New York.

Gurevich, A. V. (1961), On the theory of runaway electrons, *Sov. Phys. JETP, Engl. Transl.*, *12*(5), 904–912.

Gurevich, A. V., and K. P. Zybin (2001), Runaway breakdown and electric discharges in thunderstorms, *Phys. Uspekhi*, *44*, 1119.

Gurevich, A. V., and K. P. Zybin (2005), Runaway breakdown and the mysteries of lightning, *Phys. Today*, *58*(5), 37–43.

Gurevich, A. V., G. M. Milikh, and R. Roussel-Dupré (1992), Runaway electron mechanism of air breakdown and preconditioning during a thunderstorm, *Phys. Lett. A*, *165*, 463–468.

Gurevich, A. V., K. P. Zybin, and Y. V. Medvedev (2007), Runaway breakdown in strong electric field as a source of terrestrial gamma flashes and gamma bursts in lightning leader steps, *Phys. Lett. A*, *361*(1–2), 119–125.

Hillas, A. M. (1972), *Cosmic Rays*, Elsevier, New York.

Inan, U. S., and N. G. Lehtinen (2005), Production of terrestrial gamma-ray flashes by an electromagnetic pulse from a lightning return stroke, *Geophys. Res. Lett.*, *32*, L19818, doi:10.1029/2005GL023702.

Inan, U. S., S. C. Reising, G. J. Fishman, and J. M. Horack (1996), On the association of terrestrial gamma-ray bursts with lightning and implications for sprites, *Geophys. Res. Lett.*, *23*, 1017–1020.

Jordan, D., V. Rakov, W. Beasley, and M. Uman (1997), Luminosity characteristics of dart leaders and return strokes in natural lightning, *J. Geophys. Res.*, *102*, 22,025–22,032.

Lehtinen, N. G., M. Walt, U. S. Inan, T. F. Bell, and V. P. Pasko (1996), γ-ray emission produced by a relativistic beam of runaway electrons accelerated by quasi-electrostatic thundercloud fields, *Geophys. Res. Lett.*, *23*, 2645–2648.

Longair, M. S. (1992), *High Energy Astrophysics*, vol. 1, 2nd ed., Cambridge Univ. Press, New York.

Miki, M., V. A. Rakov, K. J. Rambo, G. H. Schnetzer, and M. A. Uman (2002), Electric fields near triggered lightning channels measured with Pockels sensors, *J. Geophys. Res.*, *107*(D16), 4277, doi:10.1029/2001JD001087.

Moore, C. B., K. B. Eack, G. D. Aulich, and W. Rison (2001), Energetic radiation associated with lightning stepped-leaders, *Geophys. Res. Lett.*, *28*, 2141–2144.

Moss, G. D., V. P. Pasko, N. Liu, and G. Veronis (2006), Monte Carlo model for analysis of thermal runaway electrons in streamer tips in transient luminous events and streamer zones of lightning leaders, *J. Geophys. Res.*, *111*, A02307, doi:10.1029/2005JA011350.

Nemiroff, R. J., J. T. Bonnell, and J. P. Norris (1997), Temporal and spectral characteristics of terrestrial gamma flashes, *J. Geophys. Res.*, *102*, 9659–9665.

Roussel-Dupré, R., and A. V. Gurevich (1996), On runaway breakdown and upward propagating discharges, *J. Geophys. Res.*, *101*, 2297–2312.

Sauli, F. (1977), Principles of operation of multiwire proportional and drift chambers, *Rep. CERN 77-09*, Eur. Org. for Nucl. Res., Geneva.

Smith, D. M., L. I. Lopez, R. P. Lin, and C. P. Barrington-Leigh (2005), Terrestrial gamma-ray flashes observed up to 20 MeV, *Science*, *307*, 1085–1088.

Williams, E., et al. (2006), Lightning flashes conducive to the production and escape of gamma radiation to space, *J. Geophys. Res.*, *111*, D16209, doi:10.1029/2005JD006447.

J. R. Dwyer, Department of Physics and Space Sciences, Florida Institute of Technology, 150 West University Boulevard, Melbourne, FL 32901, USA. (jdwyer@fit.edu)